

DEVELOPMENT OF IMAGE RECONSTRUCTION FOR DETECTING STATIC OIL-GAS REGIMES USING INVASIVE ELECTRICAL CAPACITANCE TOMOGRAPHY IN STEEL PIPE APPLICATION – AN INITIAL STUDY

Haziq Syakir Hamzah^a, Ain Eazriena Che Man^a, Yasmin Abdul Wahab^{a*}, Nurhafizah Abu Talip^{a,b}, Mohd Mawardi Saari^a

^aFaculty of Electrical and Electronics Engineering Technology, Universiti Malaysia Pahang Al-Sultan Abdullah, 26600 Pekan, Pahang, Malaysia

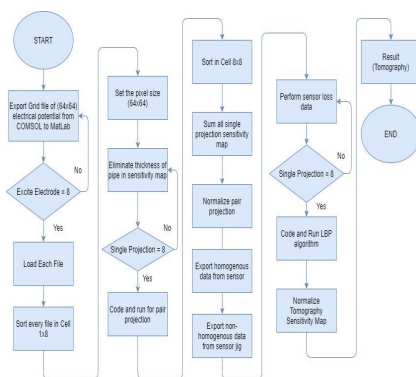
^bCenter for Research in Advanced Fluid & Processes (Fluid Centre), Universiti Malaysia Pahang Al-Sultan Abdullah, 26300 Gambang Kuantan, Malaysia

Article history

Received
19 August 2023
Received in revised form
29 October 2023
Accepted
26 November 2023
Published Online
20 April 2024

*Corresponding author
yasmin@ump.edu.my

Graphical abstract



Abstract

Electrical Capacitance Tomography (ECT) is a well-known technique for identifying two-phase regimes when a non-conducting medium is the main medium inside a pipe. However, the common non-invasive techniques of ECT are not suitable for monitoring non-conducting systems that use steel pipes. This is because the placement of the common ECT sensor is outside of the pipe and thus cannot penetrate the conducting pipe. Therefore, this paper presents the development of image reconstruction techniques for invasive Electrical Capacitance Tomography (ECT) in steel pipe applications. The study uses eight electrodes for invasive ECT that are independently designed for easy replacement. The shield guard of each electrode is individually designed, unlike the common sensor of ECT. Moreover, it produces a sensitivity map in the forward problem by modeling the geometry to mimic the real hardware of invasive ECT in Comsol Multiphysics livelink with MATLAB. The data from real hardware is exported offline and a linear back projection algorithm is used as the inverse problem. The phantom of gas-oil with different sizes, positions, and multiple phantoms from the range of 20mm, 25 mm and 33mm are tested. The tomograms of the region of interest can be obtained as a result. The paper concludes that the developed image reconstruction techniques for invasive ECT in steel pipe applications can provide acceptable and reliable results. This study can be useful for researchers and practitioners in the field of ECT and steel pipe applications.

Keywords: ECT, invasive, steel pipe, oil-gas, LBP algorithm

Abstrak

Jurnal ini membentangkan pembangunan teknik pembinaan semula imej untuk invasif Electrical Capacitance Tomography (ECT). Electrical Capacitance Tomography (ECT) ialah teknik yang terkenal untuk mengenal pasti rejim dua fasa apabila medium bukan konduktor adalah medium utama di dalam paip. Walau bagaimanapun, teknik bukan invasif biasa ECT tidak sesuai untuk memantau sistem tidak konduktor yang menggunakan paip keluli. Ini kerana penempatan elektrod ECT biasa berada di luar paip dan dengan itu tidak boleh menembusi paip pengalir. Oleh itu, jurnal ini membentangkan pembangunan teknik pembinaan semula imej untuk invasif Electrical Capacitance Tomography (ECT) dalam aplikasi

paip keluli. Kajian ini menggunakan lapan elektrod untuk ECT invasif yang direka secara bebas untuk penggantian yang mudah. Pelindung perisai setiap elektrod direka bentuk secara individu, tidak seperti elektrod ECT biasa. Selain itu, ia menghasilkan peta sensitiviti dalam masalah hadapan dengan memodelkan geometri untuk meniru perkakasan sebenar ECT invasif dalam pautan langsung Comsol Multiphysic dengan MATLAB. Data daripada perkakasan sebenar dieksport ke luar talian dan algoritma unjuran belakang linear digunakan sebagai masalah songsang. Phantom gas-minyak dengan saiz, kedudukan, dan berbilang phantom yang berbeza daripada julat 20mm, 25 mm dan 33mm diuji. Tomogram bagi kawasan yang diingini boleh diperolehi sebagai hasilnya. Makalah ini menyimpulkan bahawa teknik pembinaan semula imej yang dibangunkan untuk ECT invasif dalam aplikasi paip keluli boleh memberikan hasil yang boleh diterima dan boleh dipercayai. Kajian ini boleh berguna untuk penyelidik dan pengamal dalam bidang aplikasi ECT dan paip keluli.

Kata kunci: ECT, invasif, paip keluli, minyak-gas, algoritma LBP

© 2024 Penerbit UTM Press. All rights reserved

1.0 INTRODUCTION

Electrical Capacitance Tomography (ECT) is a powerful imaging technology that has found popularity in a variety of industrial applications. ECT uses many electrodes to detect capacitance, allowing for non-intrusive and non-invasive imaging [1]. Because of its low cost and high-speed capabilities, this imaging modality is particularly appealing for real-time monitoring in industrial settings [2], [3].

ECT, along with Electrical Resistance Tomography (ERT), is classified as a process tomography approach. Because these approaches are sensitive to passive electrical qualities such as electrical conductivity for ERT and permittivity for ECT, they are well-suited for a variety of industrial applications such as chemical engineering, food industry, and energy engineering [4]. ECT has become a vital tool in process engineering due to its ability to view and monitor flow structures, multiphase flows, and other dynamic processes in real-time.

However, in certain industrial scenarios, especially within the oil and gas industry, the use of non-intrusive ECT becomes impractical due to the prevalent use of steel pipes [7]. The reliance on steel pipes presents a unique challenge since ECT systems are traditionally non-invasive and are best suited for non-conductive materials like acrylic or Perspex tubes [1], [5], [6]. This inherent limitation prompted our research to develop an ECT system that could effectively monitor the status of non-conducting medium such as oil and gas in steel pipelines with invasive measures. The common non-invasive techniques of ECT where the sensor is located outside the pipe are not suitable for monitoring non-conducting systems that use steel pipes. This is because the placement of the common ECT will contact with the conducting pipe thus the signal cannot penetrate through the medium in the conducting pipe.

It's worth noting that the decision to employ an invasive approach comes with its own set of considerations. While invasive techniques may

introduce some degree of perturbation to the system, we have taken meticulous measures to mitigate these effects. The process of image reconstruction, as described in this paper, involves careful modeling and algorithmic solutions to ensure that the accuracy and stability of the results are maintained at a high level. Our approach aims to minimize any potential disturbances and artifacts caused by the invasive nature of the system, thus ensuring that the output remains reliable and valuable for real-time flow measurement in steel pipelines.

Moreover, the development of image reconstruction techniques for invasive ECT offers significant promise in the context of steel pipe applications. The invasive method entails using eight electrodes to measure the electrical characteristics of the steel pipe. It is possible to build a sensitivity map in the forward problem by modeling the geometry to replicate the real hardware of invasive ECT in software tools like Comsol Multiphysics with MATLAB. This map is critical for the future picture reconstruction process.

Later, the inverse problem is solved using a linear back projection technique during the image reconstruction phase. Tomograms of the region of interest can be obtained by exporting data from the real hardware and using the algorithm. To confirm the efficiency of the suggested image reconstruction approaches, phantoms of gas-oil varying in size from 20mm to 33mm were tested. The acquisition of tomograms successfully highlights the potential of invasive ECT for steel pipe applications.

In this paper, we aim to present the advancements in image reconstruction for invasive ECT in steel pipe applications. The primary goal of this work is to develop and test the image reconstruction component of the invasive ECT system. We illustrate the capability of producing precise tomograms of the region of interest by combining the capabilities of Comsol Multiphysics with MATLAB. The findings of this study add to the increasing body of knowledge in the field of ECT and provide significant insights for industry researchers and practitioners.

2.0 PRINCIPLE OF ECT

The basic concept with an ECT system is to collect capacitance changes from a multi-electrode sensor and then use that data to reconstruct a permittivity distribution. These sensors are typically composed of two electrode plates and a capacitance sensor [8], [9]. The ECT system topology is depicted in Figure 1. For image reconstruction, it normally consists of a signal generator circuit, a signal conditioning circuit, a control unit, and a computer.

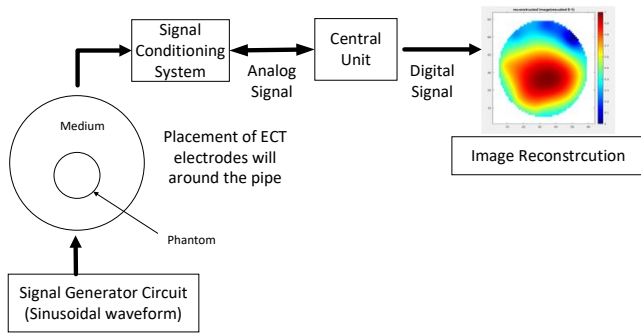


Figure 1 ECT System Topology

According to the specifications, the sensors for tomographic imaging should allow for multiple and localized measurements across a study region. To create a "body scan" of the imaging volume, numerous electrodes should be placed around its perimeter, and the capacitance between all combination pairs of electrodes should be measured [10].

Based on Figure 1, during an ECT system measurement, the initial electrode (electrode 1) acts as the excitation electrode and begins a complete cycle. All other electrodes act as receivers and measure the capacitance value that corresponds to the dielectric between them when electrode 1 is supplied with a sine wave. Capacitances between electrode 1 and electrodes 2 to last electrodes are measured in sequence. Detecting electrodes are electrodes other than electrode 1 that are at the virtual earth potential imposed by the transducer during this measurement period. Electrode 2 then becomes the source electrode, and the remaining electrodes act as detecting electrodes. The process continues until each electrode has become the source electrode, at which point the cycle is complete. The projected guards and the system screen are constantly kept at earth potential. However, in this paper only 8 electrodes are used. Thus, the independent measurement of the ECT will be based on Eq. (1) [11] and will produce 28 independent measurement data.

$$M = \frac{n(n - 1)}{2} \tag{1}$$

Table 1 illustrates how the 28 independent measurement is obtained for 8 channels of the invasive ECT system.

Table 1 Independent Measurement Sensor Data

Tx/Rx	1	2	3	4	5	6	7	8
1								
2	x							
3	x	x						
4	x	x	x					
5	x	x	x	x				
6	x	x	x	x	x			
7	x	x	x	x	x	x		
8	x	x	x	x	x	x	x	

X = sensor reading for each receiver

Besides, the number of capacitances measured independently corresponds to the number of electrode pairs measured independently. The measured capacitances are required to recreate the permittivity distribution within the vessel. The permittivity distribution influences the electric potential, according to the Poisson equation as in Eq. (2)[12]–[14].

$$\nabla \cdot (\epsilon(x,y)\nabla\phi(x,y)) = -\rho(x,y) \tag{2}$$

Whereby for two-dimensional, $\epsilon(x, y)$ is the electrical permittivity distribution, $\phi(x, y)$ is the electrical potential distribution, and $\rho(x, y)$ is the charge distribution.

3.0 METHODOLOGY

The image reconstruction process for process tomography consists of two parts: the forward problem solving and the inverse problem solving. The forward problem is used to obtain the mapping of the sensor in the pipe region, which is crucial to ensure that the sensitivity distribution is correct and represents the soft field behavior of electrical tomography[15]. The term "soft field" refers to the curving line sensitivity distribution from the excitation channel to the detection channel[16].

In addition, the inverse problem part involves implementing a suitable algorithm in getting the tomograms of the region of interest[17]. The specific algorithm used in this step depends on the choice made by the user. In this paper, we only focus on linear back projection (LBP) algorithm. Linear Back Projection is particularly well-suited for scenarios where data is collected from multiple angles or orientations, which is often the case in invasive ECT for pipeline monitoring. It allows us to reconstruct images by integrating data from various electrode positions, making it a valuable tool for visualizing the internal structures of steel pipes, even in the presence of complex geometries and materials.

To mitigate the smearing effect and optimize the resolution, our methodology incorporates advanced techniques and parameter adjustments specifically tailored to address the challenges posed by invasive ECT in steel pipe applications. These measures are designed to enhance the precision and clarity of the

reconstructed images, thereby improving the overall quality of the results.

Figure 2 shows the general steps in getting the tomograms of oil-gas regimes for invasive approach of ECT system.

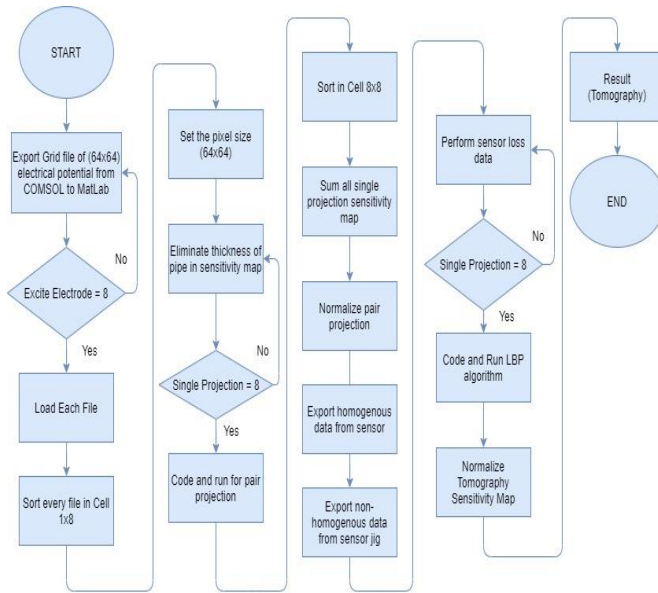


Figure 2 Flow chart of getting tomogram

The process of flowchart begins with the export of a grid file containing electrical potential data from COMSOL to MATLAB, which holds valuable information about electrical properties. The flowchart checks whether there are eight excitation electrodes; if not, it repeats the export process. If there are eight electrodes, it proceeds to load individual files, corresponding to each electrode. These files are then sorted into a 1x8 cell array for organization. The pixel size is set at 64x64, specifying the data resolution. The flowchart then eliminates data associated with the pipe's thickness in the sensitivity map to focus on internal properties.

Next, it checks for the presence of a single projection; if eight are available, the flowchart advances. The process to eliminate the pipe thickness in the sensitivity map is repeated. If there are eight single projections, the flowchart proceeds to code and run a process for pair projections. Data is organized into an 8x8 cell array, which aids data management. The sensitivity maps from single projections are summed to create a comprehensive sensitivity map.

Pair projection data is normalized to ensure uniform scaling. The flowchart then exports both homogenous and non-homogenous data from the sensor, which represent the results of these complex processing steps. Sensor data loss is addressed in a subsequent step. If eight single projections exist, an LBP algorithm is coded and run for image processing. The sensitivity map is normalized within the context of tomography, and the resulting tomography outcome is reached.

3.1 Forward Problem Solving

A sensitivity map is required for image reconstruction in every reconstruction method of an ECT system. This map serves as the foundation for combining individual pixels captured at different locations[18].

In this study, the geometry of the 8 electrodes (see Figure 3), which mimic the real pipe, was modeled using finite element model in COMSOL Multiphysics software and Livelink to MATLAB. The real sensor that attached to the inner side of steel pipe is shown in Figure 4. Table 2 shows the parameter used for the geometry model in COMSOL Multiphysics software. This allowed us to obtain the sensitivity map more easily. The electrical potential data was exported for a pixel grid of 64x64.

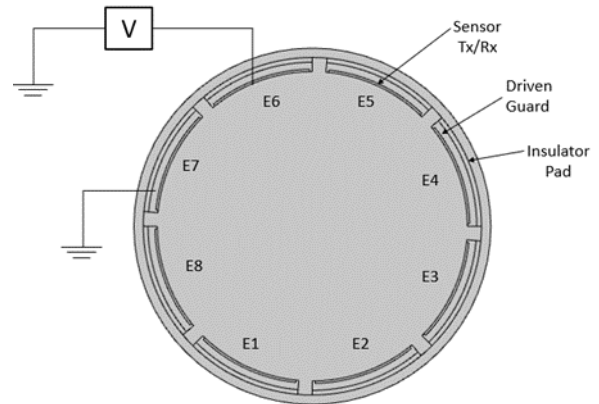


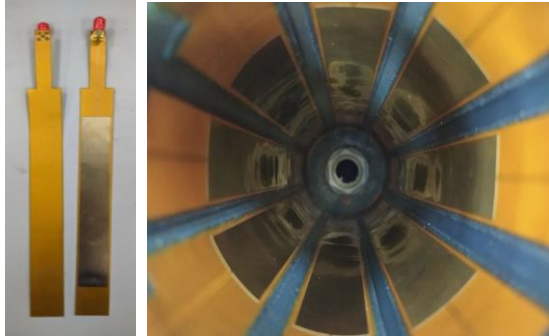
Figure 3 Geometry model of invasive ECT

Table 2 Parameter used for geometry model

Domain	Parameter	Value
Pipe	Outer diameter pipe	76mm
	Inner diameter pipe	74mm
	Thickness of pipe	2mm
	Material	Structural steel
Electrode	Relative Permittivity, ϵ_r	1
	Number of electrodes	8
	Stretch angle of electrode	40.5°
	Thickness of electrode	1mm
	Material	Copper
Insulator pad	Relative Permittivity, ϵ_r	1
	Number of insulators	8
	Stretch angle of insulator	40.5°
	Thickness of insulator	2mm
	Material	FR4
Oil	Relative Permittivity, ϵ_r	3.25
Air	Relative Permittivity, ϵ_r	1



(a)



(b)

Figure 4 Real hardware: (a) Steel pipe used, (b) Sensor used for invasive ECT and attachment inside the pipe

A 20Vpp, 150 kHz sinusoidal signal had been used as the source. We chose to use electric potential as the sensor mapping because the electrical field distribution data was too small for accurate mapping. Hence, the related formula of sensitivity map for pair electrode a and b in 2-dimensional within the area $A(x,y)$, $S_{a,b}(x,y)$ is shown in Eq. (3). The electric potential, E_a , is due to the voltage driven by electrode a, and the electric potential, E_b , is due to the voltage driven by electrode b. In other words, a and b are reflected in the electrode that acts as the excitation channel for each measurement. To obtain the pair projection of each sensitivity map, the electrical potential for each channel has been multiplied by each other.

$$S_{a,b}(x,y) = \int_{A(x,y)} \frac{E_a(x,y)}{V_a} \cdot \frac{E_b(x,y)}{V_b} \quad (3)$$

Figure 5 displays a section of code that we utilized in COMSOL Multiphysics LiveLink to MATLAB for exporting sensor distribution data.

```

for i=1:N % excitation source

model.physics('es').feature('pot1').selection.named(Sel_names(i));
model.sol('soll').runAll;

r = pixel/2; % radius

%extract data for sensitivity map
%E is 1 x N cells ( each cell size is pixelxpixel)
fprintf('extracting electrical potential map for electrode %d\n', i)%disp
V = mphinterp(model,'V','coord',grid);
V(isnan(V)) = 0;%assign NaN values as zeros
EachProj(i) = reshape(V,lx,ly);

%% eliminate the thickness of pipe

for x=1:pixel
    for y=1:pixel
        if sqrt((x-pixel/2)^2+(y-pixel/2)^2)>=r-4
            %-ve value means how much to reduce;
            %reduce pheripehry of the image by looking from the grid pixel
            EachProj(i)(x,y)=0; % set color reduced to the same color base
        end
    end
end
end
end

```

Figure 5 A part of coding to obtain sensitivity map and eliminate thickness of pipe

Since the proposed ECT approach is invasive, achieving accurate sensor mapping is crucial. Therefore, we also consider the elimination thickness of the pipe, resulting in the distribution of sensors only from the excitation channel to the detection channel, without including the thickness of the pipe. If a 64 x 64 pixel grid was exported from COMSOL, the remaining area becomes 62 x 62 pixels, with 2 pixels removed on each side of the circle.

Figure 6 shows the normalization sensitivity distribution for each pair of channels when channel 1 set as the excitation channel. The normalization of sensitivity map is done to ensure that all the data reflected to the reference image. Based on the resulting sensitivity map distribution, it is obvious that the electrode arrangement has a substantial impact on the development of sensitivity maps and that the soft field behaviour for electrical tomography is omitted. Different placements and distances between electrode pairs have been found to influence the projection path of the electrode pair.

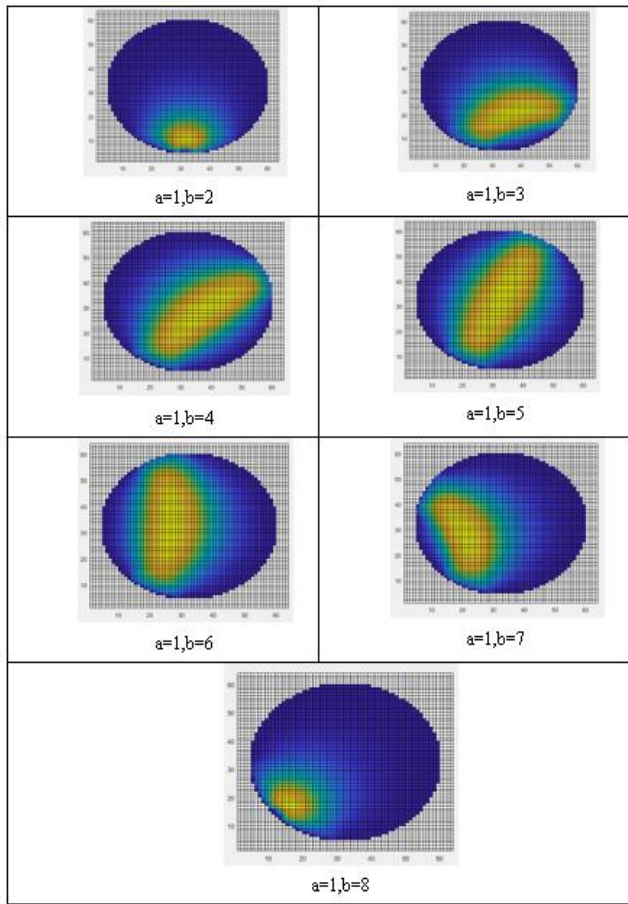


Figure 6 Sensitivity map distribution when channel 1 set as transmitter

3.2 Inverse Problem Solving

After all of the sensitivity map data has been collected, the data will be subjected to an image reconstruction procedure. Non-iterative and iterative image reconstruction techniques are the two types of image reconstruction algorithms [19]. To extract measurable data from cross-sectional images of a multiphase pipe flow, high-quality capacitance tomography data reconstruction is required.

Linear back projection (LBP) algorithm is an example of a non-iterative algorithm, which is used in this project. The simplest version of this algorithm assumes that sensitivity remains constant within the sensitivity range [20]. The LBP algorithm offers the advantage of a simpler computational method and the ability to reconstruct the image faster.

Each sensitivity matrix is multiplied by the comparable sensor reading as shown in Eq. 4. This is done to rebuild the picture using an LBP algorithm approach. To increase the data density of the projection, the back projected data values are smeared across the unknown density function (image) and overlapped. As a result, one of the most significant drawbacks of the LBP algorithm is that it

produces a blurred image, often known as the smearing effect.

$$G_{LBP}(x,y) = \sum_{a=1}^T \sum_{b=1}^R \overline{S_{a,b}(x,y)} \times V_{a,b} \quad (4)$$

Whereby the $\overline{S_{a,b}(x,y)}$ is the normalized sensitivity distribution between pair electrode and the $V_{a,b}$ is sensor loss value of sensor reading obtained from real hardware. The tomogram generated by the LBP method was normalized from 0 to 1 for simple comparison. Figure 7 presented a part of coding in MATLAB to implement the LBP algorithm and to display the tomogram.

```

***** Generating Display Map *****
%Vlbp
fprintf('reconstructing image... \n')%disp
DispMap= zeros(pixel);
for Tx=1:N
    for Rx=1:N
        DispMap= DispMap + (Attenuate_xy(Rx,Tx)*NormEpair(Rx,Tx));
    end
end
%%-----Fixed scale 0 to 1-----
normDispMap=DispMap; % rename display image
a = min(normDispMap(:));
b = max(normDispMap(:));
for Tx = 1:pixel;
    for Rx = 1:pixel;
        normDispMap(Tx,Rx) = ((normDispMap(Tx,Rx)-a) ./ (b-a))*1;
        %%eliminate NaN value at norm DispMap ; if not matlab cant plot
        %%image
        e=normDispMap(Tx,Rx);
        d=isnan(e);
        e(d)=0;
        normDispMap(Tx,Rx)=e;
    end
end
%Displaying map
f = figure('Position',[100,155,1100,370]);% position to display on the screen
subplot(1,2,1);
mpgeom(model2);
title('phantom model');

subplot(1,2,2);
pcolor(normDispMap(1:pixel,1:pixel))
%set(gca, 'Clim', [0, 255]);%use if choose imagesc to flip the image
imageCenter=[32.5,32.5];
viscircles(imageCenter,32,'EdgeColor','w','LineWidth',2); %draw circle,
title('reconstructed image(rescaled 0-1)');
shading interp; % to hide the grid line from pooler
colormap (jet) % change color map to jet colour
    
```

Figure 7 A part of coding in implementing the LBP algorithm and display tomogram

4.0 RESULTS AND DISCUSSION

In obtaining results, ECT measures variations in capacitance between electrode pairs and thereby visualizes the permittivity distribution of materials inside the sensing zone by visualizing the cross-sectional images using LBP algorithm [21]. After the measurement is taken, the mean structural similarity index (MSSIM) was employed to analyse picture performance of the ECT. The MSSIM will return a value between 0 and 1 which mean if the acquired results are high, it suggests that it is close to the reference image, and vice versa [22]. MSSIM also can serve as an objective to guide the optimization of reconstruction algorithms. By enhancing the MSSIM score, the reconstruction process can be fine-tuned to provide more accurate and faithful representations of the object under examination [23]. Thus, the results of MSSIM are helping and related to ECT in achieving better image reconstruction.

The performance of the invasive ECT system was evaluated under a range of conditions using a static PVC pipe with holes to represent gas (phantom), including different sizes, positions, and multiple sizes of phantoms. The hole pipe was made up of diameters of 20mm, 25mm, and 33mm. We used this pipe due to its limited diameter and availability in the market.

The tested phantom was started with different sizes of gases at the center of the pipe (see Figure 8). Obtaining the tomogram at the center of the pipe is crucial for electrical tomography. This is done to determine the minimum size of the phantom that can be detected. Based on Figure 8, the system is only able to detect phantom at 33mm in diameter, with an MSSIM value of 0.1472. Despite the smearing effect caused by the disadvantage of the LBP algorithm, the system was still able to detect the phantom. However, sizes smaller than 33mm do not seem to be detectable by the system. It means that the system was able to detect that the size of the phantom is around 45% of the inner diameter of the pipe.

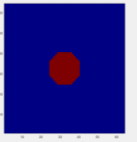
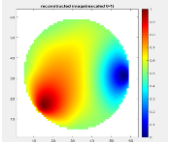
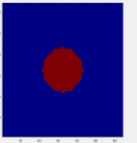
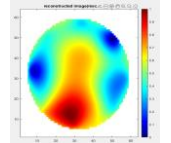
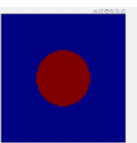
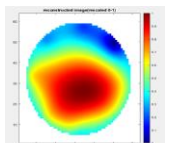
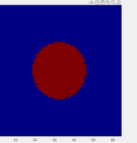
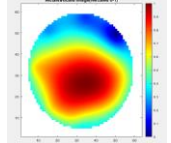
Phantom	Reference Image	Tomogram	MSSIM
20mm			0.0725
25mm			0.0985
33mm			0.1472

Figure 8 Different size of phantom at the center of the pipe

After successfully detecting an acceptable phantom using the invasive ECT system, we proceeded to test different positions of 33mm of phantom as presented in Figure 9.

Phantom	Reference Image	Tomogram	MSSIM
Center			0.1472

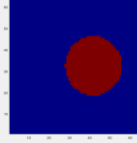
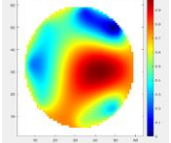
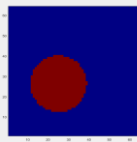
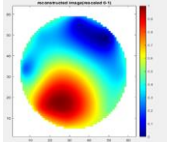
Phantom	Reference Image	Tomogram	MSSIM
Right			0.1323
Left			0.1240

Figure 9 Different positions of 33mm phantom

Based on these results obtained in Figure 9, it can be observed that the system was capable of detecting the position of the phantom in the tomogram, despite the presence of the smearing effect caused by the LBP algorithm. However, there was a decrease in the MSSIM values as the phantom was positioned further away from the center. The average MSSIM value is around 0.1345. This suggests that the accuracy and quality of the tomogram may be compromised when the gas is located away from the center. Further investigation and optimization of the algorithm may be necessary to improve the system's capability to detect smaller sizes and positions of the gas.

Lastly, we also tested multiple phantoms to further investigate the capability of the invasive ECT system (see Figure 10). It can be seen that the tomograms were blurred with the increment of the obstacle due to the smearing effect. The increment of the obstacle rose the smearing effect in LBP algorithm, hence resulting the blurriness of tomogram.

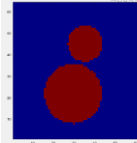
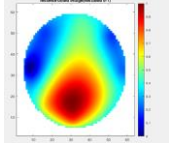
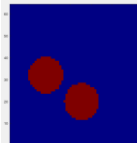
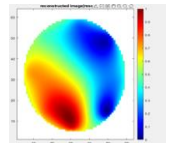
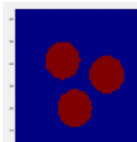
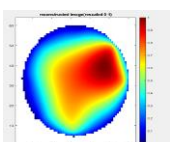
Phantom	Reference Image	Tomogram	MSSIM
20mm and 33mm			0.1623
Two 20mm			0.0895
Three 20mm			0.1443

Figure 10 Multiple phantoms

5.0 CONCLUSION

In short, the testing of the ECT model was continued with three different conditions: different sizes, positions, and multiple obstacles. It can be seen that smaller sizes and a smaller number of obstacles resulted in lower distortion. The tomogram showed good quality when the size of the obstacle was bigger. However, the LBP algorithm has some disadvantages. If the distance between the obstacle and the sensor is further, the performance of the tomogram to capture the exact position of the obstacle is lower. Additionally, the LBP algorithm creates blurry images, which is also known as the smearing effect. The increment number of obstacles in the sensor jig increased the smearing effect in the LBP algorithm, increasing the blurriness of the tomogram. Overall, the LBP algorithm was able to produce an acceptable tomography despite the smearing effect and lack of preciseness regarding obstacle position. In order to obtain more precise tomograms, we will be employing an iterative approach with a range of experiments in the future.

Conflicts of Interest

The authors declare that there is no conflict of interest regarding the publication of this paper.

Acknowledgement

The authors would like to thank Universiti Malaysia Pahang for financial support and laboratory facilities under Internal Research Grant RDU210316. Also thank to the Ministry of Higher Education for additional financial support under Fundamental Research Grant No. FRGS/1/2021/TK0/UMP/02/11 (University reference RDU210111).

References

- [1] J. Sun, W. Yang, and W. Tian. 2015. 3D Imaging based on Fringe Effect of an Electrical Capacitance Tomography Sensor. *Measurement: Journal of the International Measurement Confederation*. 74: 186-199. Doi: 10.1016/j.measurement.2015.07.018.
- [2] H. Wang and W. Yang. 2020. Application of Electrical Capacitance Tomography in Circulating Fluidised Beds – A Review. *Applied Thermal Engineering*. 176(January): 115311. Doi: 10.1016/j.applthermaleng.2020.115311.
- [3] Z. Zeeshan, C. E. Zuccarelli, D. O. Acero, Q. M. Marashdeh, and F. L. Teixeira. 2019. Enhancing Resolution of Electrical Capacitive Sensors for Multiphase Flows by Fine-stepped Electronic Scanning of Synthetic Electrodes. *IEEE Transactions on Instrumentation and Measurement*. 68(2): 462-473. Doi: 10.1109/TIM.2018.2847918.
- [4] U. Hampel et al. 2022. A Review on Fast Tomographic Imaging Techniques and Their Potential Application in Industrial Process Control. *Sensors*. 22(6). Doi: 10.3390/s22062309.
- [5] W. Deabes and K. E. Bouazza. 2021. Efficient Image Reconstruction Algorithm for ECT System Using Local Ensemble Transform Kalman Filter. *IEEE Access*. 9: 12779-12790. Doi: 10.1109/ACCESS.2021.3051560.
- [6] E. J. Mohamad, R. A. Rahim, M. H. F. Rahiman, H. L. M. Ameran, Y. A. Wahab, and O. M. F. Marwah. 2016. Analysis of Crude Palm Oil Composition in a Chemical Process Conveyor using Electrical Capacitance Tomography. *Flow Measurement and Instrumentation*. 50: 57-64. Doi: 10.1016/j.flowmeasinst.2016.06.011.
- [7] N. O. Ali, J. Mohamad-Saleh, Z. A. Aziz, and H. Talib. 2011. Optimization of Electrical Capacitance Tomography Sensor using Design of Experiment method. *Jurnal Teknologi*. 55(2): 87-99.
- [8] E. J. Mohamad, F. R. Mohd Yunus, R. Abdul Rahim, and C. K. Seong. 2011. Hardware Development of Electrical Capacitance Tomography for Imaging a Mixture of Water and Oil. *Jurnal Teknologi*. 54: 425-442.
- [9] R. Abdul Rahim. 2011. *Electrical capacitance Tomography: Principles, Techniques and Applications*. Penerbit UTM Press,
- [10] R. K. Rasel, S. M. Chowdhury, Q. M. Marashdeh, and F. L. Teixeira. 2022. Review of Selected Advances in Electrical Capacitance Volume Tomography for Multiphase Flow Monitoring. *Energies*. 15(14): 1-22. Doi: 10.3390/en15145285.
- [11] H. Herdian, I. Muffakin, A. Saputra, A. Yusuf, W. Widada, and W. P. Taruno. 2016. Hardware Implementation of Linear Back-projection Algorithm for Capacitance Tomography. *Proceedings - 2015 4th International Conference on Instrumentation, Communications, Information Technology and Biomedical Engineering, ICICI-BME 2015*. 3: 124-129. Doi: 10.1109/ICICI-BME.2015.7401348.
- [12] A. E. Che Man et al. 2023. Simulation of Frequency Selection for Invasive Approach of Electrical Capacitance Tomography for Conducting Pipe Application using Oil-gas Regimes. *Engineering Technology International Conference (ETIC 2022)*. 63-68. Doi: 10.1049/icp.2022.2571.
- [13] Y. Xu, H. Pu, Y. Li, and H. Wang. 2023. Flow Pattern Identification for Gas-oil Two-phase Flow based on a Virtual Capacitance Tomography Sensor and Numerical Simulation. *Flow Measurement and Instrumentation*. 92(March). Doi: 10.1016/j.flowmeasinst.2023.102376.
- [14] A. Voss, P. Hosseini, M. Pour-Ghaz, M. Vauhkonen, and A. Seppänen. 2019. Three-dimensional Electrical Capacitance Tomography – A Tool for Characterizing Moisture Transport Properties of Cement-based Materials. *Materials and Design*. 181: 107967. Doi: 10.1016/j.matdes.2019.107967.
- [15] Y. Abdul Wahab et al. 2018. Forward Problem Solving for Non-Invasive Electrical Resistance. *Journal of Tomography System & Sensors Application*. 1(1): 1-8.
- [16] H. L. M. Ameran et al. 2018. Sensitivity Mapping for Electrical Tomography using Finite Element Method. *International Journal of Integrated Engineering*. 10(4): 64-67.
- [17] W. Deabes, A. Sheta, K. E. Bouazza, and M. Abdelrahman. 2019. Application of Electrical Capacitance Tomography for Imaging Conductive Materials in Industrial Processes. *Journal of Sensors*. 2019(ii). Doi: 10.1155/2019/4208349.
- [18] K. Huang et al. 2019. Effect of Electrode Length of an Electrical Capacitance Tomography Sensor on Gas-Solid Fluidized Bed Measurements. *Industrial and Engineering Chemistry Research*. 58(47): 21827-21841. Doi: 10.1021/acs.iecr.9b03988.

- [19] L. Zhang and M. Zhang. 2021. Image Reconstruction of Electrical Capacitance Tomography based on Optimal Simulated Annealing Algorithm using Orthogonal Test Method. *Flow Measurement and Instrumentation*. 80(March): 101996. Doi: 10.1016/j.flowmeasinst.2021.101996.
- [20] Z. Xia, Z. Cui, Y. Chen, Y. Hu, and H. Wang. 2021. Generative Adversarial Networks for Dual-modality Electrical Tomography in Multi-phase Flow Measurement. *Measurement: Journal of the International Measurement Confederation*. 173(September 2020): 108608. Doi: 10.1016/j.measurement.2020.108608.
- [21] N. A. Abd. Rahman et al. 2018. Image Reconstruction Enhancement using Convolution Back Projection Method for Electrical Tomography Application. *International Journal of Integrated Engineering*. 10(8): 2018. Doi:10.30880/ijie.2018.10.08.015.
- [22] J. Pusppanathan et al. 2017. Single-plane Dual Modality Tomography for Multiphase Flow Imaging by Integrating Electrical Capacitance and Ultrasonic Sensors. *IEEE Sensors Journal*. 17(19): 1-1. Doi: 10.1109/JSEN.2017.2731867.
- [23] I. Bakurov, M. Buzzelli, R. Schettini, M. Castelli, and L. Vanneschi. 2022. Structural similarity index (SSIM) revisited: A data-driven approach. *Expert Systems with Applications*. 189: 116087. Doi:10.1016/j.eswa.2021.116087.